ISSN 0022-4766, Journal of Structural Chemistry, 2023, Vol. 64, No. 6, pp. 1070-1080. © Pleiades Publishing, Ltd., 2023.
Russian Text © The Author(s), 2023, published in Zhurnal Strukturnoi Khimii, 2023, Vol. 64, No. 6, 112229.

HETEROLEPTIC LANTHANIDE (La, Pr, Nd) METAL-ORGANIC FRAMEWORKS BASED ON CHLORANILIC AND FURANDICARBOXYLIC ACIDS

O. Y. Trofimova[1], A. V. Maleeva[1], K. V. Arsenyeva[1], A. V. Klimashevskaya[1], A. V. Cherkasov[1], and A. V. Piskunov[1]*

Novel heteroleptic lanthanum, praseodymium, and neodymium metal-organic coordination polymers (MOCPs) containing two types of anionic organic ligands as organic units are prepared by a two-step solvothermal synthesis in N,N-dimethylformamide. Framework derivatives with the $[Ln_2(CA)(fdc)_2 \cdot 4DMF] \cdot 2DMF$ composition are prepared (Ln = La, Pr, Nd; CA is a dianion of the chloranilic acid; fdc is a dianion of the 2,5-furandicarboxylic acid; DMF is N,N-dimethylformamide). The structure of the compounds is studied by XRD (CCDC CIF file No. 2251285 (**I**), 2251286 (**II**), 2251287 (**III**)).

DOI: 10.1134/S0022476623060100

Keywords: chloranilic acid, metal-organic coordination polymers, 2,5-furandicarboxylic acid, *redox*-active ligand, X-ray diffraction analysis, solvothermal synthesis.

INTRODUCTION

Metal-organic coordination polymers (MOCPs) are a specific class of micro- and mesoporous solids that have been widely studied for the past decades [1]. Their structural and functional diversity opens up broad prospects for applications in the fundamental and applied science [2]. Metal-organic frameworks (MOFs) have a 3D structure with some porosity and are therefore classified as a special subclass of MOCPs.

The structure and properties of MOCPs are determined both by the metal ions and by the type of organic ligands. Di-, tri- , and tetracarboxylic acids are most commonly used as ligands to build coordination polymers [3, 4]. Other promising linkers for the construction of coordination polymers are *redox*-active anilate ligands, 2,5-dihydroxy-1,4-benzoquinone derivatives, containing various substituents in positions 3 and 6 (X = H, Cl, Br, I, CN, etc.) [5-7]. Being connected with metals, these ligands can exist in four different redox states (Scheme 1). Most of the currently known MOCPs include anilate ligands in the dianionic state [6].

The use of several different ligands in a MOCP allows one to obtain compounds encompassing properties of different systems, thus paving the way to the preparation of multifunctional materials. A very promising direction in the chemistry of coordination polymers is the synthesis of heteroleptic compounds containing anionic ligands of various types in the composition of their unit [8-17]. Thus, a group of Novosibirsk researchers obtained mixed-ligand zinc derivatives (NIIC-20-G) based on dicarboxylic acids and dihydric alcohols [11-13, 16]. The authors showed that the main adsorption

[1]Razuvaev Institute of Organometallic Chemistry, Russian Academy of Sciences, Nizhny Novgorod, Russia; *pial@iomc.ras.ru. Original article submitted April 3, 2023; revised April 25, 2023; accepted April 25, 2023.

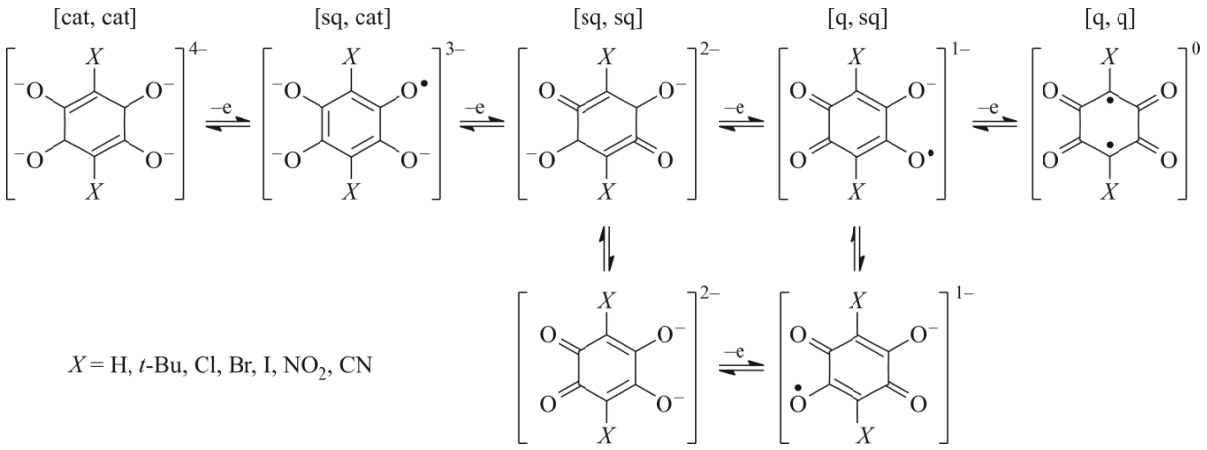

Scheme 1. Possible *redox* forms of anilate ligands.

parameters of saturated hydrocarbons (methane, ethane, and propane), which are the main components of natural gas, are affected by the size and nature of the glycol fragment in a series of zinc MOCPs [16]. These compounds also show high adsorption capacity towards various volatile organic compounds (benzene, cyclohexane, xylene isomers) [11]. Selective adsorption of NIIC-20-G compounds to various representatives of homologous series and hydrocarbon isomers allows using these frameworks for the sorption-based separation of industrially important products of petrochemical synthesis. New heteroleptic NIIC-20-G derivatives are also promising materials for air purification due to their high adsorption characteristics towards hazardous organic vapors, easy regeneration of the porous materials, and the reproducibility of their adsorption properties.

Among the huge variety of MOCPs and MOFs, lanthanide derivatives demonstrate special magnetic [18-21], luminescent [19, 22-26], sorption [27], and sensory [28, 29] properties. Recently, first examples of heteroleptic lanthanide coordination polymers based on dicarboxylate and anilate ligands were synthesized [8-10, 15]. Photophysical properties of mixed-ligand NIR-emitting Yb(III) and Er(III) derivatives make heteroleptic MOCPs [8, 10] more advantageous than their homoleptic analogs [26, 30]. The chlorocyanoanilate linker in both types of MOCPs acts as an optical antenna responsible for the Yr(III)/Er(III) luminescence sensitization as a result of efficient ligand–metal energy transfer. At the same time, the use of dicarboxylate ligands in heteroleptic systems significantly increases the efficiency of NIR radiation compared with their homoleptic counterparts. Note that the formation of end products and the phase purity of obtained derivatives directly depends on the conditions of heteroleptic MOCP synthesis [8, 9].

In the present study, we report the preparation and study of new heteroleptic lanthanide MOFs $[Ln_2(CA)(fdc)_2 \cdot 4DMF] \cdot 2DMF$ (Ln = La (**I**·2DMF), Pr (**II**·2DMF), Nd (**III**·2DMF); CA = chloranilic acid dianion; fdc = 2,5-furandicarboxylic acid dianion; DMF = N,N-dimethylformamide). The mixed-ligand derivatives were isolated from the reaction mixture in the form of finely crystalline violet samples. The structure of isostructural MOFs $[Ln_2(CA)(fdc)_2 \cdot 4DMF] \cdot 2DMF$ was studied by single-crystal XRD. Thermal stability of dried MOFs **I**–**III** was studied by thermogravimetric analysis (TGA).

EXPERIMENTAL

The IR spectra were recorded on a FSM-1201 FTIR spectrometer (suspensions in liquid paraffin; KBr pellets). The elemental analysis was performed on an Elementar Vario El cube analyzer. The TGA study was performed on a Mettler Toledo TGA/DSC3+ system at 30-700 °C in nitrogen (polycrystalline alumina crucible) at a heating rate of 5 °C/min. The following commercial reactants were used: $LaCl_3 \cdot 7H_2O$, $PrCl_3 \cdot 6H_2O$, $NdCl_3 \cdot 6H_2O$, chloranilic acid H_2CA; 2,5-furandicarboxylic acid H_2fdc; N,N′-dimethylformamide (DMF).

Synthesis of $[La_2(CA)(fdc)_2 \cdot 4DMF] \cdot 2DMF$ (**I**·2DMF), $[Pr_2(CA)(fdc)_2 \cdot 4DMF] \cdot 2DMF$ (**II**·2DMF) and $[Nd_2(CA)(fdc)_2 \cdot 4DMF] \cdot 2DMF$ (**III**·2DMF).

A mixture of one of the lanthanide salts ($LaCl_3 \cdot 7H_2O$ for **I**·2DMF, $PrCl_3 \cdot 6H_2O$ for **II**·2DMF, $NdCl_3 \cdot 6H_2O$ for **III**·2DMF, 0.04 mmol), 2,5-furandicarboxylic acid (0.08 mmol), and chloranilic acid (0.04 mmol) was ground in a mortar for better mixing of the initial materials. The resulting mixture was heated for 24 h at 80 °C in DMF (5 mL) in a sealed glass ampoule; then the temperature was increased up to 130 °C and heated for another 24 h. The isostructural MOFs **I**–**III** were obtained as purple crystalline products that were collected on a glass filter and washed with 3 mL of DMF. When dried in air, the $[Ln_2(CA)(fdc)_2 \cdot 4DMF] \cdot 2DMF$ compounds rapidly lose their crystallinity due to the gradual release of the "guest" DMF solvent from the MOF pores. For the elemental analysis, IR spectroscopy, and TGA experiments, dried samples of MOFs **I**–**III** containing no "guest" solvent were used.

Yield of MOF **I**: 72%. IR spectrum (ν, cm^{-1}): 1658 s (–C=O (DMF)), 1565 s (group –C(O)O 2,5-furandicarboxylic acid), 1487 s (–CO - CA^{2-}), 1379 s (–CO - CA^{2-}), 1295 m, 1228 w, 1200 w, 1154 w, 1112 s, 1104 s, 1066 m, 1020 s, 967 m, 867 m, 832 s, 823 s, 789 s, 976 s, 670 s, 625 m, 598 s, 576 s, 520 w, 497 s. Found (%): C 33.01, H 3.12, N 5.57; for $C_{30}H_{32}La_2Cl_2N_4O_{18}$ calculated (%): C 33.20, H 2.97, N 5.16.

Yield of MOF **II**: 70%. IR spectrum (ν, cm^{-1}): 1657 s (–C=O (DMF)), 1565 s (–C(O)O - fdc^{2-}), 1490 s (–CO - CA^{2-}), 1380 s (–CO - CA^{2-}), 1294 m, 1254 m, 1227 w, 1201 w, 1166 w, 1154 w, 1110 s, 1103 s, 1065 m, 1022 m, 991 s, 966 m, 866 m, 840 s, 823 s, 788 s, 679 s, 670 s, 625 m, 598 s, 576 s, 522 w, 498 s. Found (%): C 32.60, H 3.04, N 5.62; for $C_{30}H_{32}Pr_2Cl_2N_4O_{18}$ calculated (%): C 33.08, H 2.96, N 5.14.

Yield of MOF **III**: 63%. IR spectrum (ν, cm^{-1}): 1652 s (–C=O (DMF)), 1565 s (–C(O)O - fdc^{2-}), 1490 s (–CO - CA^{2-}), 1378 s (–CO - CA^{2-}), 1292 m, 1252 m, 1219 w, 11492 w, 1110 s, 1104 s, 1089 w, 1063 w, 1018 w, 994 m, 963 w, 866 m, 842 s, 823 s, 887 s, 678 s, 669 s, 624 m, 597 s, 577 s, 521 w, 495 s. Found (%): C 32.42, H 3.08, N 5.58; for $C_{30}H_{32}Pr_2Cl_2N_4O_{18}$ calculated (%): C 32.88, H 2.94, N 5.11.

XRD. The XRD studies of MOCPs **I**–**III** were conducted on a Bruker D8 Quest diffractometer (MoK_α radiation, ω-scanning, $\lambda = 0.71073$ Å, $T = 100.0(2)$ K). The measurements and integrations of experimental intensities, absorption corrections, structure determination and refinements were carried out using APEX3 [31], SADABS [32], and SHELX [33] packages. The structures were determined using the dual-space algorithm [34] and refined by full-matrix least squares on F^2_{hkl} anisotropically for the non-hydrogen atoms. All hydrogen atoms in **I**–**III** were calculated geometrically and refined isotropically with fixed thermal parameters $U(H)_{iso} = 1.2U(C)_{eq}$ ($U(H)_{iso} = 1.5U(C)_{eq}$ for methyl groups).

The topology of coordination polymers was analyzed using the ToposPro software [35].

The structures were deposited with the Cambridge Crystallographic Data Centre (CCDC numbers 2251285 (**I**), 2251286 (**II**), 2251287 (**III**)) and are available at ccdc.cam.ac.uk/structures.

RESULTS AND DISCUSSION

Heteroleptic lanthanide MOFs $[Ln_2(CA)(fdc)_2 \cdot 4DMF] \cdot 2DMF$ (Ln = La (**I**·2DMF), Pr (**II**·2DMF), Nd (**III**·2DMF)) were prepared by a previously developed technique [9] using two-stage solvothermal synthesis (Scheme 2). At the first stage, the reaction mixture was heated up to 80 °C for 24 h; at the second stage, the thermostat temperature increased to 130 °C, and the reaction mixture was heated for another 24 h. As a result, purple crystalline mixed-ligand MOCPs were obtained. The purple color of the crystals is not unusual for such derivatives and is typical for compounds containing anilate ligands in the dianion state [14].

The structure of **I**·2DMF, **II**·2DMF, and **III**·2DMF was determined by XRD. The **I**·2DMF, **II**·2DMF, and **III**·2DMF MOCPs are isostructural, so their structure was considered on the example of the **I**·2DMF derivative. The molecular structure of **I**·2DMF is shown in Fig. 1. The crystal data and parameters of XRD experiments for isostructural MOCPs $[Ln_2(CA)(fdc)_2 \cdot 4DMF] \cdot 2DMF$ (La, Pr, Nd) are summarized in Table 1; the selected bond lengths are listed in Table 2.

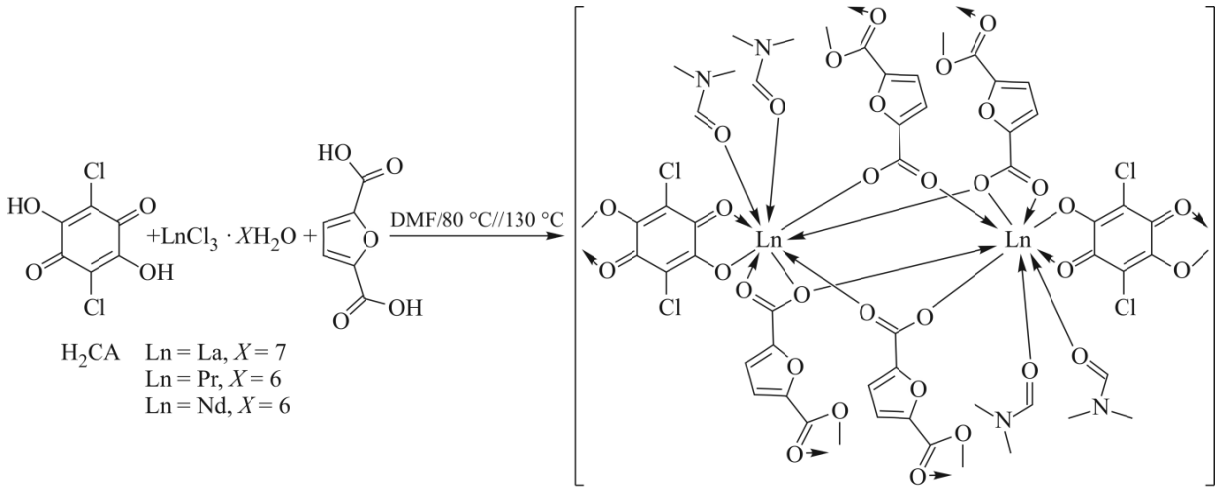

Scheme 2. Synthesis of MOCPs **I**–**III**.

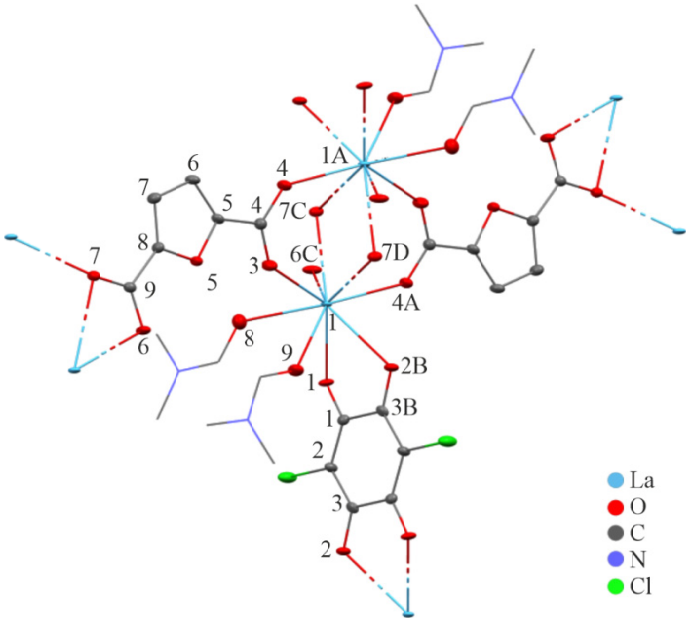

Fig. 1. Molecular structure of the **I**·2DMF unit. Color code of the atoms: La (cyan), C (grey), O (red), N (purple) (see the electronic version). Thermal ellipsoids are set at a 50% probability level. Hydrogen atoms and "guest" DMF molecules are not shown.

According to the XRD data, the **I**·2DMF, **II**·2DMF, and **III**·2DMF derivatives are isostructural and crystallize in the $P2_1/c$ monoclinic space group. The formal coordination number of metal centers in these compounds is nine: La^{3+} (**I**), Pr^{3+} (**II**), and Nd^{3+} (**III**) cations are bonded to five oxygen atoms of four fdc^{2-} dianions, two oxygen atoms of CA^{2-} dianions, and two oxygen atoms of two coordinated DMF molecules (Fig. 1). The structural unit of each MOCP is formed by two metal centers connected to each other by means of two μ_2–κ^1:κ^1-bridging COO groups of furandicarboxylic acids and participates in the formation of secondary building units (Fig. 2*a*). The distance between two Ln atoms in the secondary building units of **I**·2DMF, **II**·2DMF, and **III**·2DMF is 4.0713(3) Å, 4.0044(4) Å, and 3.9790(5) Å, respectively. There are two uncoordinated

TABLE 1. Crystal Data, Experimental Parameters, and Structure Refinements for **I**·2DMF, **II**·2DMF, **III**·2DMF

Parameter	**I**·2DMF	**II**·2DMF	**III**·2DMF
Empirical formula	$C_{30}H_{32}ClLaN_4O_{18}$, $2C_3H_7NO$	$C_{30}H_{32}ClPrN_4O_{18}$, $2C_3H_7NO$	$C_{30}H_{32}ClNdN_4O_{18}$, $2C_3H_7NO$
M	1231.51	1235.51	1242.17
T, K	100.0(2)	100.0(2)	100.0(2)
Crystal system	Monoclinic		
Space group	$P2_1/c$		
a, b, c, Å	12.4745(4), 11.1476(4), 16.9373(6)	12.3434(7), 11.1718(7), 16.8162(10)	12.3034(6), 11.2273(8), 16.7297(11)
β, deg	94.7390(10)	94.337(2)	94.172(5)
V, Å^3	2347.26(14)	2312.3(2)	2304.8(3)
Z	2	2	2
ρ_{calc}, g/cm^3	1.742	1.775	1.790
μ, mm^{-1}	1.991	2.281	2.427
θ_{min} / θ_{max}, deg	2.67 / 27.95	2.19 / 25.03	2.456 / 25.96
Reflections collected / unique ($I > 2\sigma(I)$)	22288 / 4798	21394 / 3420	21798 / 4505
R_{int}	0.0370	0.0569	0.0563
$S(F^2)$	1.038	1.039	1.085
R_1 / wR_2 ($F^2 > 2\sigma(F^2)$)	0.0253 / 0.0553	0.0327 / 0.0542	0.0386 / 0.0924
R_1 / wR_2 (all data)	0.0340 / 0.0527	0.0420 / 0.0561	0.0512 / 0.0999
$\Delta\rho_{max}$ / $\Delta\rho_{min}$, e/Å^3	0.82 / –0.99	1.28 / –1.15	2.13 / –0.89

solvate DMF molecules per each MOCP unit. The MOCP 2D layers in **I**·2DMF, **II**·2DMF, and **III**·2DMF are built due to the μ_2–κ^1:κ^2 bonds between free COO groups of the fdc^{2-} dianions and metal cations of the neighboring units (Fig. 2*b*). Finally, the chloranilic acid dianions "crosslink" the layers into a 3D non-interpenetrating structure with the xah topology [35-37] (Fig. 2*c*).

MOCPs with anilate [38-40] and dicarboxylate [41] ligands can show different types of coordination for the metal atom; most common of them are shown in Scheme 3 on the example of chloranil and 2,5-furandicarboxylic acids. The types of ligand coordination in **I**·2DMF, **II**·2DMF, and **III**·2DMF are shown in the scheme by rectangles.

The structure of chloranilic acid dianions in **I**·2DMF, **II**·2DMF, and **III**·2DMF can be represented as two delocalized π-electronic OCCCO systems connected by single C–C bonds. The lengths of single C–C bonds range from 1.537(3) Å to 1.546(4) Å (Table 2), while other C–C distances of the six-membered rings fall within a wider range of 1.382(7)-1.408(7) Å. The lengths of the C–O bonds (1.249(4)-1.257(5) Å) are intermediate between single and double C–O bonds [42].

As already shown, dicarboxylate ligands in all derivatives act as bridging μ_2–κ^1:κ^1 and μ_2–κ^1:κ^2 ligands connecting four Ln^{3+} ions. The La–O (2.509(2)-2.695(2) Å). Pr–O (2.462(2)-2.652(2) Å), and Nd–O (2.462(2)-2.632(2) Å) bonds fall within the intervals typical for La, Pr, and Nd MOCPs with 2,5-furandicarboxylic acid [43, 44].

The pores in the crystal structures of **I**·2DMF, **II**·2DMF, and **III**·2DMF have a volume of 22% and are occupied by DMF guest molecules (Fig. 3) [45]. The crystal lattice destroys when the guest molecules are released and the pores are emptied. For example, when stored without mother solvent in air for 24 h, the **I**·2DMF, **II**·2DMF, and **III**·2DMF samples lose their crystallinity to the extent that their powder XRD spectra show no distinct diffraction peaks. The elemental analysis and TGA data confirm the absence of DMF guest molecules in the dried samples and show agree well with the results for the simplest formula $[Ln_2(CA)(fdc)_2 \cdot 4DMF]$ (La, Pr, Nd).

TABLE 2. Selected Bond Lengths (Å) in **I**·2DMF, **II**·2DMF, **III**·2DMF

Bond *d*, Å	**I**·2DMF	Bond *d*, Å	**II**·2DMF	Bond *d*, Å	**III**·2DMF
La1–O1	2.501(2)	Pr1–O1	2.458(2)	Nd1–O1	2.442(3)
La1–O7$^{\#4}$	2.507(2)	Pr1–O3	2.473(2)	Nd1–O4$^{\#1}$	2.444(3)
La1–O4$^{\#1}$	2.509(2)	Pr1–O4A	2.462(2)	Nd1–O7$^{\#4}$	2.452(3)
La1–O3	2.509(2)	Pr1–O7D	2.465(2)	Nd1–O3	2.466(3)
La1–O9	2.543(2)	Pr1–O9	2.500(2)	Nd1–O9	2.477(3)
La1–O8	2.553(2)	Pr1–O2B	2.534(2)	Nd1–O8	2.491(3)
La1–O2$^{\#2}$	2.568(2)	Pr1–O8	2.508(2)	Nd1–O2$^{\#1}$	2.524(3)
La1–O6$^{\#3}$	2.596(2)	Pr1–O6C	2.562(2)	Nd1–O6$^{\#3}$	2.544(3)
La1–O7$^{\#3}$	2.695(2)	Pr1–O7C	2.652(2)	Nd1–O7$^{\#3}$	2.632(3)
La1–La1$^{\#1}$	4.0713(3)	Pr1–Pr1A	4.0044(4)	Nd1–Nd1$^{\#3}$	3.9790(5)
O1–C1	1.257(3)	O1–C1	1.255(4)	O1–C1	1.257(5)
O2–C3	1.253(3)	O2–C3	1.252(4)	O2–C3	1.249(6)
O3–C4	1.257(3)	O3–C4	1.260(4)	O3–C4	1.261(6)
O4–C4	1.256(3)	O4–C4	1.257(4)	O4–C4	1.258(6)
O6–C9	1.248(3)	O6–C9	1.244(4)	O6–C9	1.243(6)
O7–C9	1.278(3)	O7–C9	1.287(4)	O7–C9	1.284(5)
C1–C2	1.389(3)	C1–C2	1.388(4)	C1–C2	1.382(7)
C1–C3$^{\#2}$	1.537(3)	C1–C3B	1.546(4)	C1–C3$^{\#2}$	1.538(6)
C2–C3	1.400(3)	C2–C3	1.391(5)	C2–C3	1.408(7)
C4–C5	1.487(3)	C4–C5	1.498(4)	C4–C5	1.490(7)
C5–C6	1.360(3)	C5–C6	1.351(4)	C5–C6	1.352(6)
C6–C7	1.420(3)	C6–C7	1.420(4)	C6–C7	1.416(7)
C7–C8	1.363(3)	C7–C8	1.357(4)	C7–C8	1.359(6)
C8–C9	1.475(3)	C8–C9	1.472(4)	C8–C9	1.477(6)

Symmetry operators: $^{\#1}$ $-x+1, -y+1, -z+2$; $^{\#2}$ $-x+2, -y+1, -z+2$; $^{\#3}$ $x, -y+3/2, z+1/2$; $^{\#4}$ $-x+1, y-1/2, -z+3/2$.

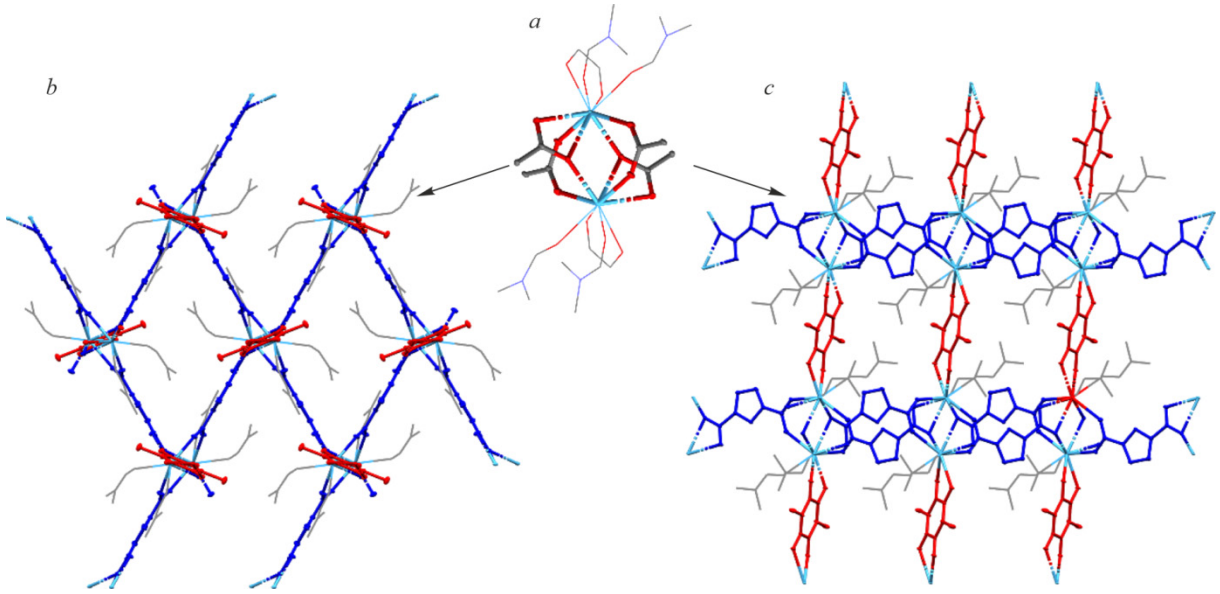

Fig. 2. Secondary building unit in **I**·2DMF (*a*). View of the **I**·2DMF framework along direction (100) (*b*) and (010) (*c*). Color code: La (cyan), chloranilic acid dianion (red), 2,5-furandicarboxylic acid dianion (blue), DMF (gray) (see the electronic version). Thermal ellipsoids are set at a 50% probability level Hydrogen atoms and "guest" DMF molecules are not shown.

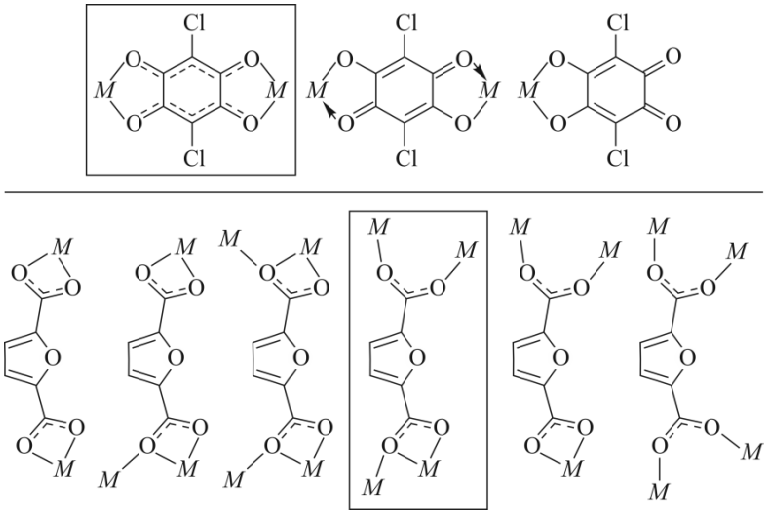

Scheme 3. Possible types of the coordination of anionic ligands.

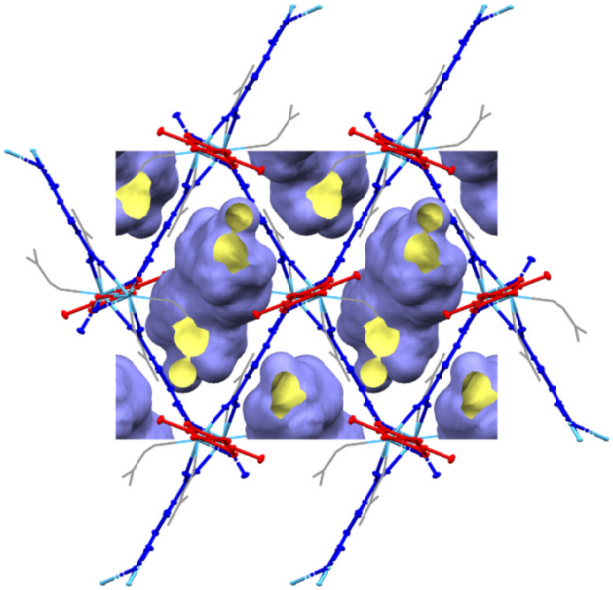

Fig. 3. Pores in the crystal packing of **I**·2DMF as viewed along the (100) direction (probe radius: 1.2 Å, step: 0.7 Å). The outer and inner pore surfaces are shown purple and yellow, respectively (see the electronic version).

The TGA data indicate that the anionic framework of $[Ln_2(CA)(fdc)_2 \cdot 4DMF]$ (**I**–**III**) is thermally quite stable (Fig. 4). The TGA curve shows that the dried MOFs contain no guest solvent. All the derivatives show four successive steps of weight loss corresponding to the stepwise removal of four coordinated DMF molecules from the lanthanide ions. In the case of the lanthanum MOF (**I**), the steps 2-4 are not pronounced, but the weight loss of 21% corresponds to three coordinated DMF molecules. More exact data on the temperature intervals and weight losses for all the compounds are presented in Table 3. The anionic framework of the derivatives begins to destroy above 320 °C. Thermal stability of the heteroleptic MOCPs **I**–**III** is close to that of homoleptic (anilate and carboxylate) derivatives of lanthanides [43, 46].

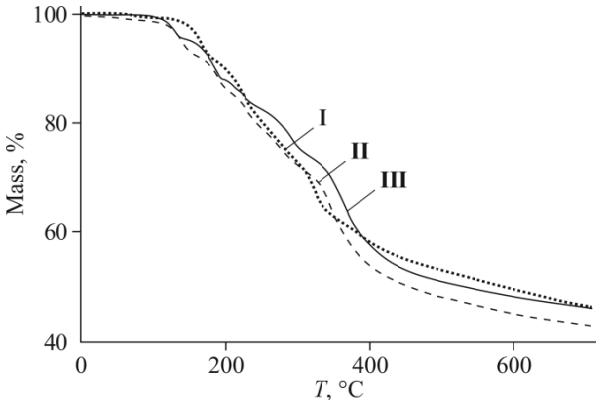

Fig. 4. Thermogravimetric curves for the MOFs **I**–**III**.

TABLE 3. TGA Data for **I**–**III**

ΔT_1, °C / weight loss, %		
I	**II**	**III**
150-190 / 7	135-180 / 7	140-175 / 6
190-320 / 21	180-225 / 7	175-225 / 8
	225-270 / 7	225-275 / 6
	270-320 / 7	275-320 / 8

CONCLUSIONS

New mixed-ligand MOFs of lanthanides (La, Pr, Nd) containing two types of anionic ligands (anilate and dicarboxylate) in the composition of their units were described. According to the XRD data, the obtained compounds are isostructural 3D coordination polymers containing solvate dimethylformamide molecules in their pores. The loss of the latter during the drying of crystalline samples results in the crystallinity loss. The TGA data indicate that the anionic framework of the synthesized lanthanide MOFs destroys above 320 °C.

ADDITIONAL INFORMATION

The study was carried out using the equipment of the Analytical Center of IOMC RAS.

FUNDING

This work was funded the Russian Science Foundation (project No. 22-23-00750).

CONFLICT OF INTERESTS

The authors declare that they have no conflicts of interests.

REFERENCES

1. K. A. Kovalenko, A. S. Potapov, and V. P. Fedin. Micro- and mesoporous metal-organic frameworks for hydrocarbon separation. *Russ. Chem. Rev.*, **2022**, *91*, RCR5026. https://doi.org/10.1070/RCR5026

2. M. A. Agafonov, E. V. Alexandrov, N. A. Artyukhova, G. E. Bekmukhamedov, V. A. Blatov, V. V. Butova, Y. M. Gayfulin, A. A. Gharibyan, Z. N. Gafurov, Y. G. Gorbunova, L. G. Gordeeva, M. S. Gruzdev, A. N. Gusev, G. L. Denisov, D. N. Dybtsev, Y. Y. Enakieva, A. A. Kagilev, A. O. Kantyukov, M. A. Kiskin, K. A. Kovalenko, A. M. Kolker, D. I. Kolokolov, Y. M. Litvinova, A. A. Lysova, N. V. Maksimchuk, Y. V. Mironov, Y. V. Nelyubina, V. V. Novikov, V. I. Ovcharenko, A. V. Piskunov, D. M. Polyukhov, V. A. Polyakov, V. G. Ponomarev, A. S. Poryvaev, G. V. Romanenko, A. V. Soldatov, M. V. Solovyov, A. G. Stepanov, I. V. Terekhov, O. Y. Trofimova, V. P. Fedin, M. V. Fedin, O. A. Holdeeva, A. Y. Tsivadze, W. V. Chervonova, A. I. Cherevko, V. F. Shulgin, E. S. Shutov, and D. G. Yakhvarov. Metal-organic coordination polymers in Russia: From synthesis and structure to functional properties and materials. *J. Struct. Chem.*, **2022**, *63*(5), 671. https://doi.org/10.26902/JSC_id93211
3. B. Li, H.-M. Wen, Y. Cui, W. Zhou, G. Qian, and B. Chen. Emerging multifunctional metal-organic framework materials. *Adv.Mater.*, **2016**, *28*, 8819. https://doi.org/10.1002/adma.201601133
4. H. Jiang, D. Alezi, and M. Eddaoudi. A reticular chemistry guide for the design of periodic solids. *Nat. Rev. Mater.*, **2021**, *6*, 466. https://doi.org/10.1038/s41578-021-00287-y
5. S. Kitagawa and S. Kawata. Coordination compounds of 1,4-dihydroxybenzoquinone and its homologues. Structures and properties. *Coord. Chemi. Rev.*, **2002**, *224*, 11. https://doi.org/10.1016/S0010-8545(01)00369-1
6. N. Monni, M. Oggianu, S. A. Sahadevan, and M. L. Mercuri. Redox activity as a powerful strategy to tune magnetic and/or conducting properties in benzoquinone-based metal-organic frameworks. *Magnetochemistry*, **2021**, *7*, 109. https://doi.org/10.3390/magnetochemistry7080109
7. N. Monni, M. S. Angotzi, M. Oggianu, S. A. Sahadevan, and M. L. Mercuri. Redox-active benzoquinones as challenging “non-innocent” linkers to construct 2D frameworks and nanostructures with tunable physical properties. *J. Mater. Chem. C*, **2022**, *10*, 1548. https://doi.org/10.1039/d1tc05335c
8. S. A. Sahadevan, F. Manna, A. Abhervé, M. Oggianu, N. Monni, V. Mameli, D. Marongiu, F. Quochi, F. Gendron, B. L. Guennic, N. Avarvari, and M. L. Mercuri. Combined experimental/theoretical study on the luminescent properties of homoleptic/heteroleptic erbium(III) anilate-based 2D coordination polymers. *Inorg. Chem.*, **2021**, *60*, 17765. https://doi.org/10.1021/acs.inorgchem.1c02386
9. O. Y. Trofimova, A. V. Maleeva, I. V. Ershova, A. V. Cherkasov, G. K. Fukin, R. R. Aysin, K. A. Kovalenko, and A. V. Piskunov. Heteroleptic La^{III} anilate/dicarboxylate based neutral 3D-coordination polymers. *Molecules*, **2021**, *26*, 2486. https://doi.org/10.3390/molecules26092486
10. S. A. Sahadevan, N. Monni, M. Oggianu, A. Abhervé, D. Marongiu, M. Saba, A. Mura, G. Bongiovanni, V. Mameli, C. Cannas, N. Avarvari, F. Quochi, and M. L. Mercuri. Heteroleptic NIR-emitting Yb^{III}/anilate-based neutral coordination polymer nanosheets for solvent sensing. *ACS Appl. Nano Mater.*, **2020**, *3*, 94. https://doi.org/10.1021/acsanm.9b01740
11. A. A. Lysova, K. A. Kovalenko, D. N. Dybtsev, S. N. Klyamkin, E. A. Berdonosova, and V. P. Fedin. Hydrocarbon adsorption in a series of mesoporous metal-organic frameworks. *Microporous Mesoporous Mater.*, **2021**, *328*, 111477. https://doi.org/10.1016/j.micromeso.2021.111477
12. A. A. Lysova, D. G. Samsonenko, K. A. Kovalenko, A. S. Nizovtsev, D. N. Dybtsev, and V. P. Fedin. A series of mesoporous metal-organic frameworks with tunable windows sizes and exceptionally high ethane over ethylene adsorption selectivity. *Angew. Chem., Int. Ed.*, **2020**, *59*, 20561. https://doi.org/10.1002/anie.202008132
13. A. A. Lysova, D. G. Samsonenko, P. V. Dorovatovskii, V. A. Lazarenko, V. N. Khrustalev, K. A. Kovalenko, D. N. Dybtsev, and V. P. Fedin. Tuning the molecular and cationic affinity in a series of multifunctional metal-organic frameworks based on dodecanuclear Zn(II) carboxylate wheels. *J. Am. Chem. Soc.*, **2019**, *141*, 17260. https://doi.org/10.1021/jacs.9b08322
14. O. Y. Trofimova, A. V. Maleeva, K. V. Arsenyeva, A. V. Klimashevskaya, I. A. Yakushev, and A. V. Piskunov. Glycols in the synthesis of zinc-anilato coordination polymers. *Crystals*, **2022**, *12*, 370. https://doi.org/10.3390/cryst12030370

15. M. Oggianu, F. Manna, S. A. Sahadevan, N. Avarvari, A. Abhervé, and M. L. Mercuri. Metal-organic framework vs. coordination polymer–influence of the lanthanide on the nature of the heteroleptic anilate/terephtalate 3D network. *Crystals*, **2022**, *12*, 763. https://doi.org/10.3390/cryst12060763
16. A. A. Lysova, K. A. Kovalenko, A. S. Nizovtsev, D. N. Dybtsev, and V. P. Fedin. Efficient separation of methane, ethane and propane on mesoporous metal-organic frameworks. *Chem. Eng. J.*, **2023**, *453*, 139642. https://doi.org/10.1016/j.cej.2022.139642
17. S. Benmansour, C. Pintado-Zaldo, J. Martínez-Ponce, A. Hernández-Paredes, A. Valero-Martínez, M. Gómez-Benmansour, and C. J. Gómez-García. The versatility of ethylene glycol to tune the dimensionality and magnetic properties in Dy^{III}-anilato-based single-ion magnets. *Cryst. Growth Des.*, **2023**, *23*, 1269. https://doi.org/10.1021/acs.cgd.2c01409
18. P. J. Saines and N. C. Bristowe. Probing magnetic interactions in metal-organic frameworks and coordination polymers microscopically. *Dalton Trans.*, **2018**, *47*, 13257. https://doi.org/10.1039/c8dt02411a
19. S. Benmansour, C.J. Gómez-García. Lanthanoid-anilato complexes and lattices. *Magnetochemistry*, **2020**, *6*, 71. https://doi.org/10.3390/magnetochemistry6040071
20. P. Gómez-Claramunt, S. Benmansour, A. Hernández-Paredes, C. Cerezo-Navarrete, C. Rodríguez-Fernández, J. Canet-Ferrer, A. Cantarero, and C. J. Gómez-García. Tuning the structure and properties of lanthanoid coordination polymers with an asymmetric anilato ligand. *Magnetochemistry*, **2018**, *4*, 6. https://doi.org/10.3390/magnetochemistry4010006
21. K. Bondaruk and C. Hua. Effect of counterions on the formation and structures of Ce(III) and Er(III) chloranilate frameworks. *Cryst. Growth Des.*, **2019**, *19*, 3338. https://doi.org/10.1021/acs.cgd.9b00233
22. T. Gorai, W. Schmitt, and T. Gunnlaugsson. Highlights of the development and application of luminescent lanthanide based coordination polymers, MOCPs and functional nanomaterials. *Dalton Trans.*, **2021**, *50*, 770. https://doi.org/10.1039/d0dt03684f
23. M. D. Allendorf, C. A. Bauer, R. K. Bhakta, and R. J. T. Houk. Luminescent metal–organic frameworks. *Chem. Soc. Rev.*, **2009**, *38*, 1330. https://doi.org/10.1039/b802352m
24. M. Huangfu, M. Wang, C. Lin, J. Wang, and P. Wu. Luminescent metal–organic frameworks as chemical sensors based on “mechanism–response”: a review. *Dalton Trans.*, **2021**, *50*, 3429. https://doi.org/10.1039/D0DT04276E
25. P. A. Demakov, A. A. Vasileva, V. A. Lazarenko, A. A. Ryadun, and V. P. Fedin. Crystal structures, thermal and luminescent properties of gadolinium(III) trans-1,4-cyclohexanedicarboxylate metal-organic frameworks. *Crystals*, **2021**, *11*, 1375. https://doi.org/10.3390/cryst11111375
26. S. A. Sahadevan, N. Monni, A. Abhervé, D. Marongiu, V. Sarritzu, N. Sestu, M. Saba, A. Mura, G. Bongiovanni, C. Cannas, F. Quochi, N. Avarvari, and M. L. Mercuri. Nanosheets of two-dimensional neutral coordination polymers based on near-infrared-emitting lanthanides and a chlorocyananilate ligand. *Chem. Mater.*, **2018**, *30*, 6575. https://doi.org/10.1021/acs.chemmater.8b03399
27. C. J. Kingsbury, B. F. Abrahams, J. E. Auckett, H. Chevreau, A. D. Dharma, S. Duyker, Q. He, C. Hua, T. A. Hudson, K. S. Murray, W. Phonsri, V. K. Peterson, R. Robson, and K. F. White. Square grid metal–chloranilate networks as robust host systems for guest sorption. *Chem. Eur. J.*, **2019**, *25*, 5222. https://doi.org/10.1002/chem.201805600
28. H.-H. Zeng, W.-B. Qiu, L. Zhang, R.-P. Liang, and J.-D. Qiu. Lanthanide coordination polymer nanoparticles as an excellent artificial peroxidase for hydrogen peroxide detection. *Anal. Chem.*, **2016**, *88*, 6342. https://doi.org/10.1021/acs.analchem.6b00630
29. H.-J. Chen, L.-Q. Chen, L.-R. Lin, L.-S. Long, and L.-S. Zheng. Doped luminescent lanthanide coordination polymers exhibiting both white-light emission and thermal sensitivity. *Inorg. Chem.*, **2021**, *60*, 6986. https://doi.org/10.1021/acs.inorgchem.1c00740
30. F. Artizzu, M. Atzori, J. Liu, D. Mara, K. V. Hecke, and R. V. Deun. Solution-processable Yb/Er 2D-layered metallorganic frameworks with high NIR-emission quantum yields. *J. Mater. Chem. C*, **2019**, *7*, 11207. https://doi.org/10.1039/c9tc03698a

31. APEX3; SAINT. Madison, Wisconsin, USA: Bruker AXS Inc., **2018**.
32. L. Krause, R. Herbst-Irmer, G. M. Sheldrick, and D. Stalke. Comparison of silver and molybdenum microfocus X-ray sources for single-crystal structure determination. *J. Appl. Crystallogr.*, **2015**, *48*, 3. https://doi.org/10.1107/S1600576714022985
33. G. M. Sheldrick. Crystal structure refinement with SHELXL. *Acta Crystallogr*., *Sect. C: Struct. Chem.*, **2015**, *71*(1), 3-8. https://doi.org/10.1107/s2053229614024218
34. G. M. Sheldrick. SHELXT - Integrated space-group and crystal-structure determination. *Acta Crystallogr*., *Sect. A: Found. Adv.*, **2015**, *71*(1), 3-8. https://doi.org/10.1107/s2053273314026370
35. V. A. Blatov, A. P. Shevchenko, and D. M. Proserpio. Applied topological analysis of crystal structures with the program package ToposPro. *Cryst. Growth Des.*, **2014**, *14*, 3576. https://doi.org/10.1021/cg500498k
36. E. V. Alexandrov, V. A. Blatov, A. V. Kochetkov, and D. M. Proserpio. Underlying nets in three-periodic coordination polymers: topology, taxonomy and prediction from a computer-aided analysis of the Cambridge Structural Database. *CrystEngComm*, **2011**, *13*, 3947. https://doi.org/10.1039/c0ce00636j
37. E. V. Alexandrov, A. P. Shevchenko, N. A. Nekrasova, and V. A. Blatov. Topological methods for analysis and design of coordination polymers. *Russ. Chem. Rev*., **2022**, *91*, RCR5032. https://doi.org/10.1070/RCR5032
38. S. Benmansour, G. López-Martínez, J. Canet-Ferrer, and C. J. Gómez-García. A family of lanthanoid dimers with nitroanilato bridges. *Magnetochemistry*, **2016**, *2*, 32. https://doi.org/10.3390/magnetochemistry2030032
39. L. A. Dubraja, K. Molcanov, D. Zilic, B. Kojic-Prodic, and E. Wenger. Multifunctionality and size of the chloranilate ligand define the topology of transition metal coordination polymers. *New J.Chem.*, **2017**, *41*, 6785. https://doi.org/10.1039/c7nj01058c
40. V. Vuković, K. I. Molčanov, C. Jelsch, E. Wenger, A. Krawczuk, M. Jurić, L. A. Dubraja, and B. Kojić-Prodić. Malleable electronic structure of chloranilic acid and its species determined by X-ray charge density studies. *Cryst. Growth Des.*, **2019**, *19*, 2802. https://doi.org/10.1021/acs.cgd.9b00033
41. H.-Y. Cao, Q.-Y. Liu, M.-J. Gao, Y.-L. Wang, L.-L. Chen, and Y. Liu. Ionothermal syntheses, crystal structures and luminescence of three three-dimensional lanthanide-1,4-benzenedicarboxylate frameworks. *Inorg. Chim. Acta*, **2014**, *414* 226. https://doi.org/10.1016/j.ica.2014.02.014
42. S. N. Brown. Metrical oxidation states of 2-amidophenoxide and catecholate ligands: Structural signatures of metal–ligand π bonding in potentially noninnocent ligands. *Inorg. Chem.*, **2012**, *51*, 1251. https://doi.org/10.1021/ic202764j
43. H. Wang, R.-M. Wen, and T.-L. Hu. Two series of lanthanide metal-organic frameworks constructed from crown-ether-like secondary building units. *Eur. J. Inorg. Chem.*, **2014**, *2014*, 1185. https://doi.org/10.1002/ejic.201301324
44. Ya-PingWang, X.-Y. Li, H.-H. Li, H.-Z. Zhang, H.-Y. Sun, Q. Guo, H. Li, and Z. Niu. A novel 3D Nd(III) metal-organic frameworks based onfuran-2,5-dicarboxylic acid exhibits new topology and rare near-infrared luminescence property. *Inorg. Chem. Commun.*, **2016**, *70*, 27. https://doi.org/10.1016/j.inoche.2016.05.008
45. L. J. Barbour. Crystal porosity and the burden of proof. *Chem. Commun.*, **2006**, (11), 1163. https://doi.org/10.1039/B515612M
46. A. D. Kharitonov, O. Yu. Trofimova, I. N. Meshcheryakova, G. K. Fukin, M. N. Khrizanforov, Y. H. Budnikova, A. S. Bogomyakov, R. R. Aysin, K. A. Kovalenko, and A. V. Piskunov. 2D-Metal-organic coordination polymers of lanthanides (La(III), Pr(III) and Nd(III)) with redox-active dioxolene bridging ligand. *CrystEngComm*, **2020**, *22*, 4675. https://doi.org/10.1039/d0ce00767f